Journal of Alloys and Compounds 488 (2009) L21–L25

Contents lists available at ScienceDirect

Journal of Alloys and Compounds

journal homepage: www.elsevier.com/locate/jallcom

Letter

Hydrogen sensors made of undoped and Pt-doped SnO_2 nanowires

Yanbai Shen, Toshinari Yamazaki*, Zhifu Liu, Dan Meng, Toshio Kikuta

Faculty of Engineering, University of Toyama, 3190 Gofuku, Toyama 930-8555, Japan

ARTICLE INFO

Article history:
Received 11 May 2009
Available online 31 August 2009

Keywords:
Tin oxide
Nanowires
Gas sensor
Hydrogen
Platinum

ABSTRACT

Tin oxide (SnO_2) nanowires with a tetragonal structure were formed on oxidized Si substrates by thermal evaporation of tin grains at 900 °C. The morphology, crystal structure, and H_2 gas sensing properties of undoped and Pt-doped SnO_2 nanowires were investigated. SnO_2 nanowires were approximately 30–200 nm in diameter and several tens of micrometers in length. Gas sensors made of undoped, 0.8 wt% Pt-doped, and 2 wt% Pt-doped SnO_2 nanowires showed a reversible response to H_2 at an operating temperature of RT–300 °C. The sensitivity increased with increasing H_2 concentration. The highest sensitivity of 118 was obtained for 2 wt% Pt-doped SnO_2 nanowire sensor to 1000 ppm H_2 at an operating temperature of 100 °C. The gas sensing properties of Pt-doped and Pd-doped SnO_2 nanowires were also investigated to compare the effect of impurity doping. The results demonstrated that impurity doping improved the sensitivity and lowered the operating temperature at which the sensitivity was maximized.

1. Introduction

It appears that hydrogen (H_2) will play an important role as a clean and abundant energy source in the near future. H_2 produces only water on combustion and provides zero emission [1,2]. However, H_2 is dangerous for transport and storage because it is flammable and explosive and also because it easily leaks from gas-handling equipments if handled carelessly. Therefore, it is essential to develop high-performance H_2 gas sensors for domestic and industrial applications.

Many studies on the development of gas sensors that utilize changes in the resistance of oxide semiconductors, such as SnO_2 [3–7], ZnO [8–10], and WO_3 [11,12], have been carried out. Recently, it was reported that quasi-one-dimensional nanomaterials such as nanowires, nanobelts, and nanotubes showed high sensitivity, quick response, and enhanced ability to detect gases at low concentrations because of their high surface-to-volume ratio, single crystalline structure, and great surface activity [10,13–16]. Of these nanomaterials, quasi-one-dimensional SnO_2 has been extensively studied. For examples, Comini et al. [6,14] reported that SnO_2 nanowires and nanobelts were sensitive to environmental polluting species, such as CO, NO_2, and ethanol, at operating temperatures above 200 °C. Xue et al. [17] reported that indium-doped SnO_2 nanowires showed a high response to ethanol at a temperature of 400 °C. Qian et al. [18] reported that Au-decorated SnO_2 nanobelts showed a high sensitivity to CO and the sensitivity increased with increasing CO concentration at operating temperatures of 250–400 °C. Although the SnO_2 nanowires have been investigated as gas sensing materials as mentioned above, these studies have mostly dealt with operation at a high temperature. However, the operation at a high temperature results in high power consumption and complexity in integration, which limits the application of SnO_2 gas sensors. Thus, we determined to investigate the gas sensing properties at various temperatures including room temperature. In the present study, we studied the formation, microstructure, and H_2 sensing properties of undoped and Pt-doped SnO_2 nanowires. It was found that Pt doping not only improved the sensitivity to H_2 but also decreased the operating temperature at which the sensitivity was maximized. These results indicated a possibility of developing a gas sensor made of SnO_2 nanowires operable at a low temperature with low power consumption.

2. Experimental

SnO_2 nanowires were formed on oxidized Si substrates by thermal evaporation of tin grains. The apparatus used for the formation of SnO_2 nanowires is illustrated in Fig. 1(a). Tin grains 1 mm in diameter with a purity of 99.9% were placed on oxidized Si substrates in an alumina boat. No catalysts and impurities were introduced. The alumina boat was placed at the center of a quartz tube inserted in a horizontal tube furnace. Argon gas at a flow rate of 50 ml/min was introduced into the quartz tube at ambient pressure. The furnace was heated to 900 °C and kept at this temperature for 1 h. A layer of wire-shaped products was obtained on the substrates around the tin grains after cooling down of the furnace to room temperature.

Gas sensors made of SnO_2 nanowires were fabricated by pouring a few drops of nanowire-suspended ethanol onto oxidized Si substrates equipped with a pair of interdigitated Pt electrodes with a gap length of 0.12 mm. The structure of an SnO_2 nanowire sensor is shown in Fig. 1(b). The weight of SnO_2 nanowires dispersed on a substrate was approximately 0.5 mg and the area of sensing element was 7 mm × 10 mm. In the doping of platinum, 40-μl ethanol solution of platinic

* Corresponding author. Tel.: +81 764456882; fax: +81 764456882.
E-mail address: yamazaki@eng.u-toyama.ac.jp (T. Yamazaki).

0925-8388/$ – see front matter © 2009 Elsevier B.V. All rights reserved.
doi:10.1016/j.jallcom.2009.08.124

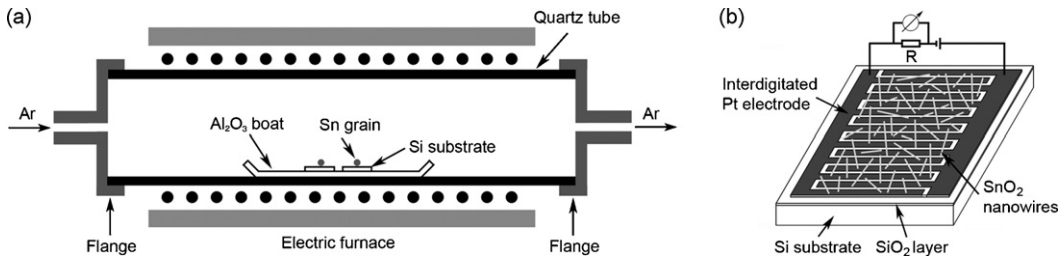

Fig. 1. (a) Apparatus used for the formation of SnO_2 nanowires. (b) Structure of an SnO_2 nanowire sensor.

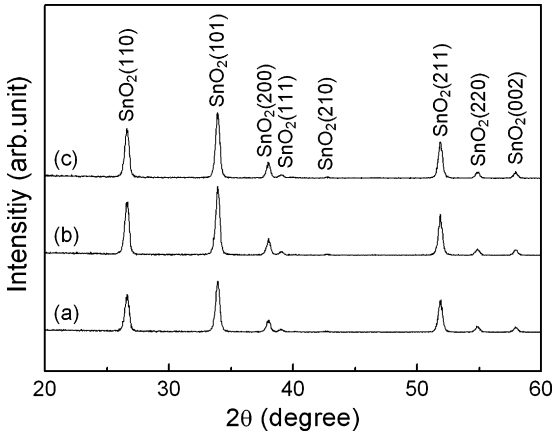

Fig. 2. XRD patterns of undoped and Pt-doped SnO_2 nanowires after annealing at 350 °C for 30 min in air. (a) Undoped SnO_2 nanowires. (b) 0.8 wt% Pt-doped SnO_2 nanowires. (c) 2 wt% Pt-doped SnO_2 nanowires.

chloride ($H_2PtCl_6{\cdot}6H_2O$) with a concentration of 5×10^{-4} or 1.25×10^{-3} mol/l was poured onto SnO_2 nanowire sensors. After annealing at 350 °C for 30 min in air, three types of gas sensors were fabricated: undoped, 0.8 wt% Pt-doped, and 2 wt% Pt-doped SnO_2 nanowire sensors. The Pt concentration in the Pt-doped sensors was estimated by calculating the weight ratio of Pt in ethanol solution of platinic chloride to SnO_2 nanowires. The structure of undoped and Pt-doped SnO_2 nanowires was investigated by using an X-ray diffractometer (XRD) (Shimadzu XRD-6100) with Cu Kα radiation, a field emission scanning electron microscope (FE-SEM) (JEOL JSM-6700F), and a transmission electron microscope (TEM) (JEOL EM002B) equipped with an energy dispersive X-ray spectrometer (EDX).

H_2 gas sensing properties were measured in a quartz tube that was inserted in an electric furnace. The operating temperature was varied from room temperature (RT = 25 °C) to 300 °C by heating the furnace. Dry synthetic air was introduced in the quartz tube at a flow rate of 200 ml/min. When the sensitivity of the sensors was measured, a small amount of hydrogen was added at a desired concentration to the synthetic air. The electrical resistance of gas sensors was determined by measuring the electric current that flowed when a potential difference of 10 V was applied between the interdigitated Pt electrodes. In this study, the sensitivity was defined

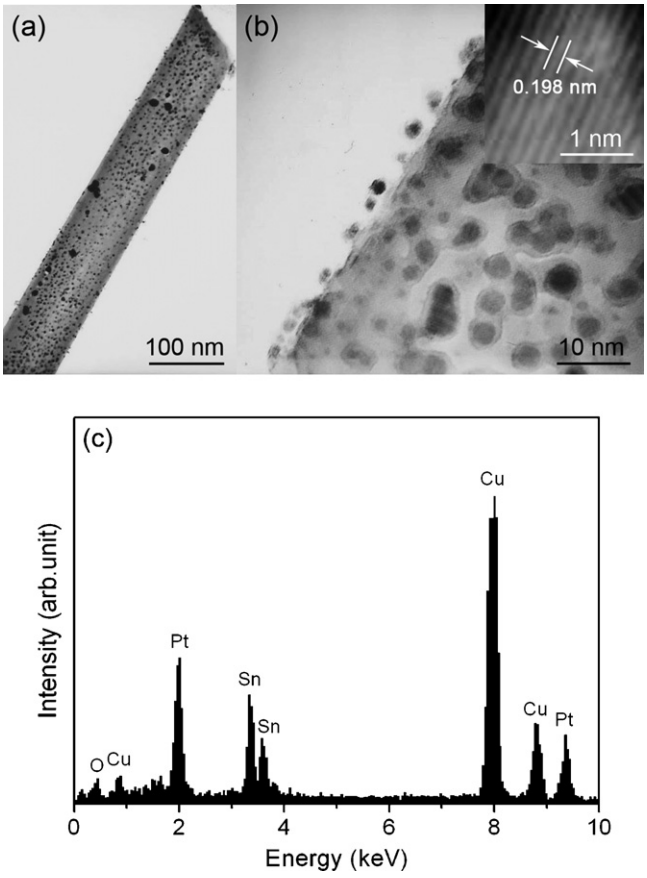

Fig. 4. (a) TEM image of a 2 wt% Pt-doped SnO_2 nanowire with a diameter of 88 nm. (b) HRTEM image of the nanowire. The inset is the enlarged HRTEM image for a Pt particle on the nanowire. (c) EDX analysis of the nanowire.

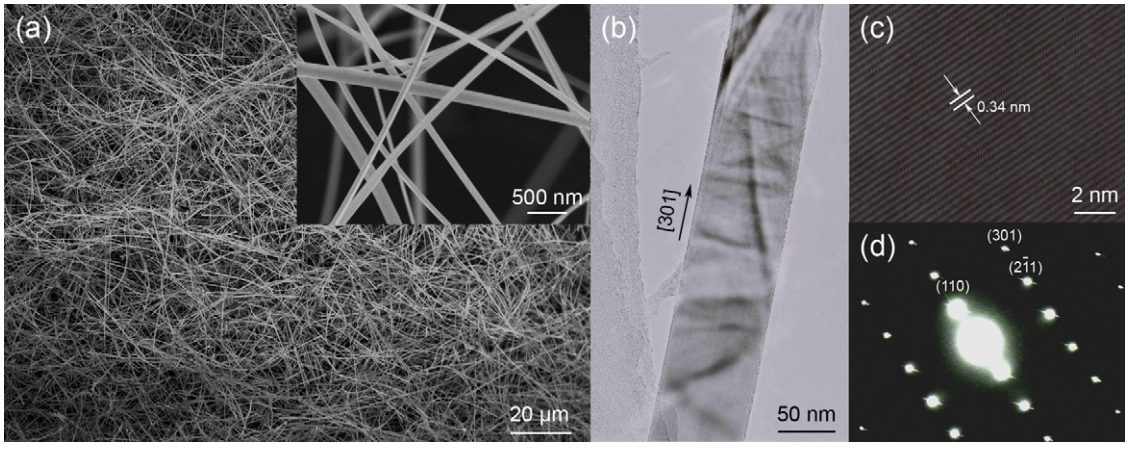

Fig. 3. (a) FE-SEM image of undoped SnO_2 nanowires. The inset is a high magnification FE-SEM image. (b) TEM image of an undoped SnO_2 nanowire with a diameter of 90 nm. (c) HRTEM image of the nanowire. (d) SAED pattern of the nanowire.

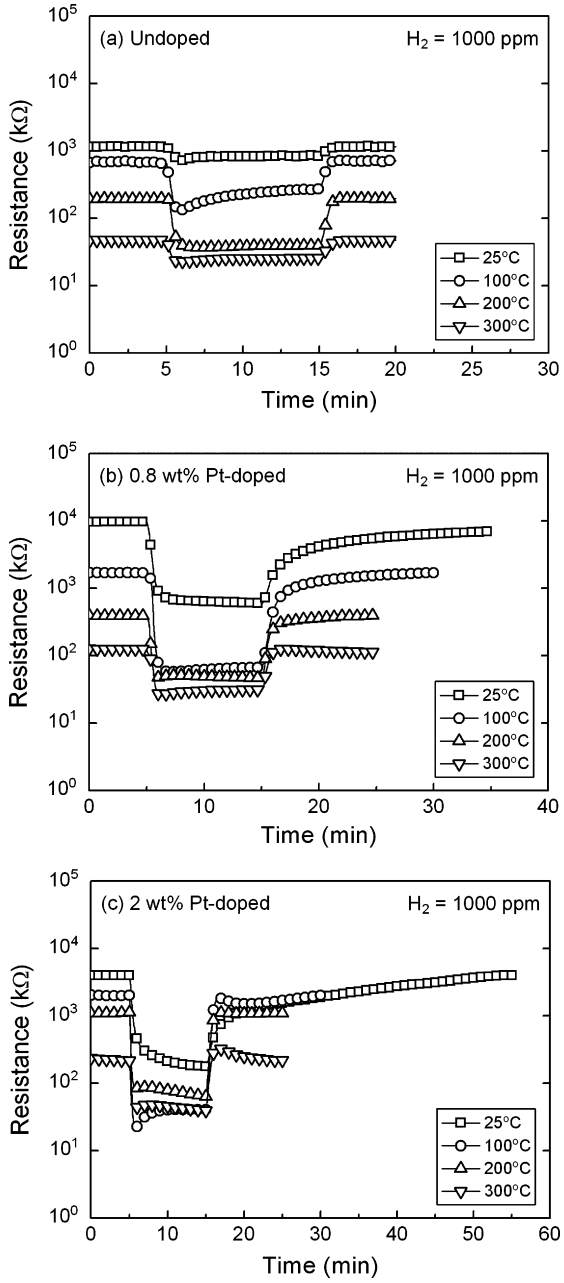

Fig. 5. Changes in the resistances of the undoped and Pt-doped SnO_2 nanowire gas sensors upon exposure to 1000 ppm H_2 at different operating temperatures. (a) Undoped SnO_2 nanowires. (b) 0.8 wt% Pt-doped SnO_2 nanowires. (c) 2 wt% Pt-doped SnO_2 nanowires.

as $(R_a - R_g)/R_g$, where R_a was the electrical resistance before the introduction of H_2, and R_g was the minimum electrical resistance after the introduction of H_2.

3. Results and discussion

The XRD patterns observed for undoped and Pt-doped SnO_2 nanowires after annealing at 350 °C for 30 min in air are shown in Fig. 2. The undoped SnO_2 nanowires are identified as a tetragonal SnO_2 in JCPDS card No. 41-1445. As it is shown later by TEM observation, Pt particles are formed in Pt-doped SnO_2 nanowires. However, Pt peaks are not observed in XRD patterns probably because Pt concentrations are low.

A typical FE-SEM image of undoped SnO_2 nanowires is shown in Fig. 3(a). The inset shows a high magnification FE-SEM image. The SnO_2 nanowires are 30–200 nm in diameter and several tens

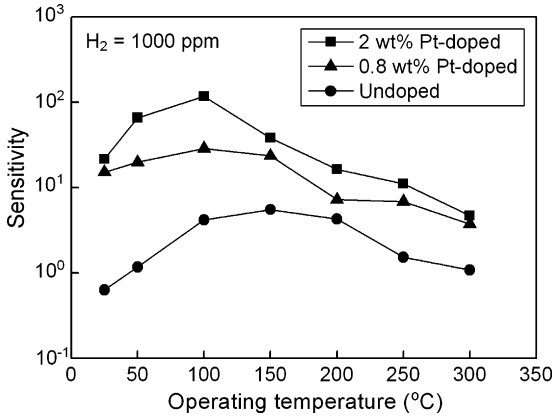

Fig. 6. Sensitivities of the undoped and Pt-doped SnO_2 nanowire sensors upon exposure to 1000 ppm H_2 at various operating temperatures.

of micrometers in length. A TEM image of an undoped nanowire with a diameter of 90 nm is shown in Fig. 3(b). A high-resolution TEM (HRTEM) image of this nanowire and the selected area electron diffraction (SAED) pattern shown in Fig. 3(c) and (d) indicate that the nanowire is a single crystal. The interplanar spacing of 0.34 nm shown in Fig. 3(c) corresponds to the (1 1 0) plane in a tetragonal SnO_2 structure. The growth direction of SnO_2 nanowires is [3 0 1] as indicated in Fig. 3(b), which is consistent with previous reports [19,20].

A TEM image of a 2 wt% Pt-doped SnO_2 nanowire with a diameter of 88 nm is shown in Fig. 4(a). Pt particles, which appear as dark spots, are distributed randomly on the surface of the SnO_2 nanowire. The corresponding HRTEM image (Fig. 4(b)) shows that Pt particles are 1–6 nm in diameter. The inset in Fig. 4(b) is an enlarged HRTEM image for one particle. The interplanar spacing of 0.198 nm corresponding to (2 0 0) plane of fcc Pt indicates that the dark spots are metallic Pt particles. EDX analysis of this nanowire (Fig. 4(c)) indicates that SnO_2 nanowires are surely doped with Pt.

Typical changes in the resistance of the sensors made of undoped, 0.8 wt% Pt-doped, and 2 wt% Pt-doped SnO_2 nanowires upon exposure to 1000 ppm H_2 measured at different operating temperatures are shown in Fig. 5(a)–(c), respectively. At every operating temperature, the resistance decreases upon exposure to H_2 and completely recovers to the initial value after the removal of H_2. It should be noted that the recovery time is shorter than 2 min for the undoped sensor even at room temperature. The sensitivity is greatly improved by Pt doping. Although the recovery time increases with the doping of Pt, it is shorter than 40 min.

The sensitivities are summarized in Fig. 6 as a function of the operating temperature for three types of gas sensors upon exposure to 1000 ppm H_2. The sensitivity of the undoped sensor is relatively low, and the maximum sensitivity is 5.5 at 150 °C. As the Pt concentration increases, the sensitivity increases and the operating temperature at which the sensitivity shows a maximum is lowered to 100 °C. The highest sensitivity of 118 is observed in this study for the 2 wt% Pt-doped sensor at an operating temperature of 100 °C. We see that Pt doping not only improves the sensitivity but also lowers the operating temperature at which the sensitivity is maximized. It should be noted that two sensor samples were fabricated for each type of the sensor, and H_2 gas sensing properties of these two samples were found to be similar, indicating a good reproducibility. The improvement on the sensitivity of the Pt-doped sensors is ascribed to the effect of "chemical sensitization mechanism" proposed by Yamazoe et al. [21]. Pt particles catalytically activate the dissociation of hydrogen molecules by a "spillover" effect, forming atomic hydrogen. The atomic hydrogen diffuses to the surface of SnO_2 nanowires, which activates the

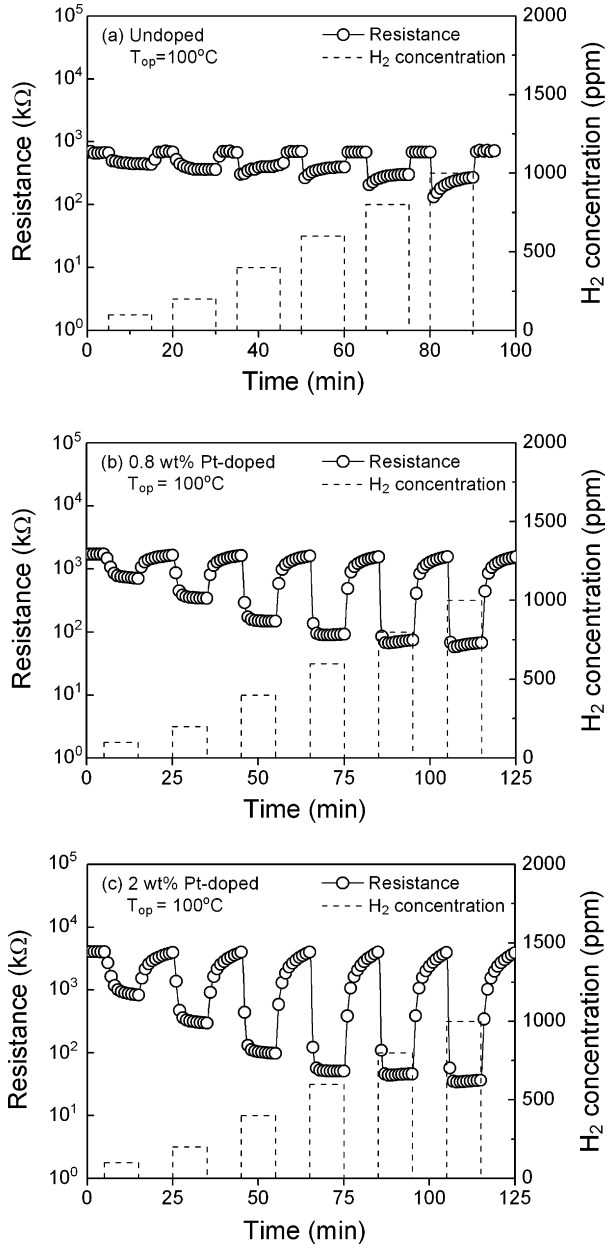

Fig. 7. Changes in the resistances of the undoped and Pt-doped SnO_2 nanowire sensors measured at an operating temperature of 100 °C. The measurement was performed for various H_2 concentrations. (a) Undoped SnO_2 nanowires. (b) 0.8 wt% Pt-doped SnO_2 nanowires. (c) 2 wt% Pt-doped SnO_2 nanowires.

reaction between hydrogen and the adsorbed oxygen [21,22]. This results in an effective shrinkage of the depletion layer at the surface of nanowires and lowers the resistance of the Pt-doped sensors, leading to a high sensitivity.

The changes in the resistance of the undoped and Pt-doped sensors at an operating temperature of 100 °C are shown in Fig. 7(a)–(c). The measurement of the sensitivity was performed for various H_2 concentrations of 100–1000 ppm. In every sensor, the resistance decreases upon exposure to H_2. The decrease in the resistance is enhanced with increasing H_2 concentration. The resistance shows a good reversibility during the cycles of introduction and exhaust of H_2. The change in the resistance of the undoped sensor upon exposure to H_2 is relatively small (Fig. 7(a)). The change in the resistance is greatly enhanced by the doping of 0.8 wt% Pt (Fig. 7(b)). For the 2 wt% Pt-doped sensor (Fig. 7(c)), the sensitivities upon exposure to 100, 200, 400, 600, 800, and 1000 ppm H_2 are 4, 12, 41, 78, 91, and 118, respectively.

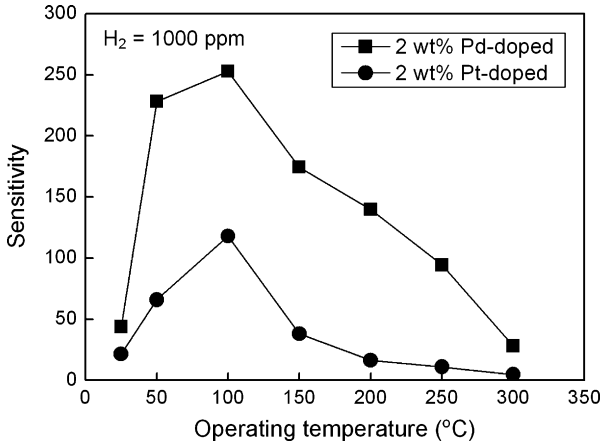

Fig. 8. Sensitivities of Pt-doped and Pd-doped SnO_2 nanowires to 1000 ppm H_2 as a function of the operating temperature.

In the previous work, we also reported the H_2 gas sensing properties of Pd-doped SnO_2 nanowires [13]. To investigate the effect of impurity doping on gas sensing properties, the sensitivities of Pt-doped and Pd-doped SnO_2 nanowires to 1000 ppm H_2 are represented in Fig. 8 as a function of the operating temperature. The highest sensitivity of Pd-doped nanowires was also obtained at 100 °C. It can be seen that the sensitivities of Pd-doped SnO_2 nanowires are higher than those of Pt-doped SnO_2 nanowires, especially in the temperature range of 50–250 °C. The difference in the sensing properties of two types of impurity-doped nanowires may be taken into account the chemical state of impurity. In the case of Pt doping, Pt particles are distributed on the surface of SnO_2 nanowires. As mentioned above, the sensitivity is improved by the effect of "chemical sensitization mechanism", namely "spillover effect". However, in the case of Pd doping, PdO particles are formed in air and reduced to metallic Pd in H_2, resulting in the electron transfer between PdO/Pd particles and SnO_2. In this way, the sensitivity is greatly enhanced by two effects of "chemical sensitization mechanism" and "electronic sensitization mechanism" [21,22]. Therefore, the sensitivity of Pd-doped nanowires is highly improved compared with that of Pt-doped nanowires.

4. Conclusions

SnO_2 nanowires with a tetragonal structure were formed on oxidized Si substrates by thermal evaporation of tin grains at 900 °C. SnO_2 nanowires of a single crystal structure were approximately 30–200 nm in diameter and several tens of micrometers in length. Pt particles of 1–6 nm in diameter were randomly distributed on the surface of Pt-doped SnO_2 nanowires. Gas sensors made of undoped SnO_2 nanowires, 0.8 wt% Pt-doped SnO_2 nanowires, and 2 wt% Pt-doped SnO_2 nanowires showed a reversible response to H_2 at an operating temperature of RT–300 °C. The sensitivity increased with increasing Pt concentration. The highest sensitivity obtained in this study upon exposure to 1000 ppm H_2 was 118, which was measured at 100 °C for a sensor made of 2 wt% Pt-doped SnO_2 nanowires. Pt doping improved the sensitivity and lowered the operating temperature at which the sensitivity was maximized. The gas sensing properties of Pt-doped and Pd-doped SnO_2 nanowires were also investigated to compare the effect of impurity doping. This result indicates the potential of impurity-doped SnO_2 nanowires for developing gas sensors operable at a low temperature with low power consumption.

Acknowledgement

The authors wish to thank Dr. T. Kawabata for his cooperation in TEM measurements.

References

[1] S. Shukla, S. Seal, L. Ludwig, C. Parish, Sens. Actuators B 97 (2004) 256–265.
[2] Y.B. Shen, T. Yamazaki, Z.F. Liu, C.J. Jin, T. Kikuta, N. Nakatani, Thin Solid Films 516 (2008) 5111–5117.
[3] V. Jayaraman, K.I. Gnanasekar, E. Prabhu, T. Gnanasekaran, G. Periaswami, Sens. Actuators B 55 (1999) 147–153.
[4] T. Yamazaki, H. Okumura, C.J. Jin, A. Nakayama, T. Kikuta, N. Nakatani, Vacuum 77 (2005) 237–243.
[5] S.G. Ansari, P. Boroojerdian, S.R. Sainkar, R.N. Karekar, R.C. Aiyer, S.K. Kulkarni, Thin Solid Films 295 (1997) 271–276.
[6] E. Comini, G. Faglia, G. Sberveglieri, Z.W. Pan, Z.L. Wang, Appl. Phys. Lett. 81 (2002) 1869–1871.
[7] A. Kolmakov, Y.X. Zhang, G.S. Cheng, M. Moskovits, Adv. Mater. 15 (2003) 997–1000.
[8] H.Y. Xu, X.L. Liu, D.L. Cui, M. Li, M.H. Jiang, Sens. Actuators B 114 (2006) 301–307.
[9] L.C. Tien, P.W. Sadik, D.P. Norton, L.F. Voss, S.J. Pearton, H.T. Wang, B.S. Kang, F. Ren, J. Jun, J. Lin, Appl. Phys. Lett. 87 (2005) 222106.
[10] H.T. Wang, B.S. Kang, F. Ren, L.C. Tien, P.W. Sadik, D.P. Norton, S.J. Pearton, J. Lin, Appl. Phys. Lett. 86 (2005) 243503.
[11] D. Davazoglou, T. Dritsas, Sens. Actuators B 77 (2001) 359–362.
[12] M. Gillet, K. Aguir, M. Bendahan, P. Mennini, Thin Solid Films 484 (2005) 358–363.
[13] Y.B. Shen, T. Yamazaki, Z.F. Liu, D. Meng, T. Kikuta, N. Nakatani, M. Saito, M. Mori, Sens. Actuators B 135 (2009) 524–529.
[14] E. Comini, G. Faglia, G. Sberveglieri, D. Calestani, L. Zanotti, M. Zha, Sens. Actuators B 111–112 (2005) 2–6.
[15] A. Vomiero, S. Bianchi, E. Comini, G. Faglia, M. Ferroni, N. Poli, G. Sberveglieri, Thin Solid Films 515 (2007) 8356–8359.
[16] P.C. Xu, Z.X. Cheng, Q.Y. Pan, J.Q. Xu, Q. Xiang, W.J. Yu, Y.L. Chu, Sens. Actuators B 130 (2008) 802–808.
[17] X.Y. Xue, Y.J. Chen, Y.G. Liu, S.L. Shi, Y.G. Wang, T.H. Wang, Appl. Phys. Lett. 88 (2006) 201907.
[18] L.H. Qian, K. Wang, Y. Li, H.T. Fang, Q.H. Lu, X.L. Ma, Mater. Chem. Phys. 100 (2006) 82–84.
[19] Y.Q. Chen, X.F. Cui, K. Zhang, D.Y. Pan, S.Y. Zhang, B. Wang, J.G. Hou, Chem. Phys. Lett. 369 (2003) 16–20.
[20] J.X. Wang, D.F. Liu, X.Q. Yan, H.J. Yuan, L.J. Ci, Z.P. Zhou, Y. Gao, L. Song, L.F. Liu, W.Y. Zhou, G. Wang, S.S. Xie, Solid State Commun. 130 (2004) 89–94.
[21] N. Yamazoe, Y. Kurokawa, T. Seiyama, Sens. Actuators B 4 (1983) 283–289.
[22] S. Matsushima, Y. Teraoka, N. Miura, N. Yamazoe, Jpn. J. Appl. Phys. 27 (1988) 1798–1802.